Partial Interdigitation of Lipid Bilayers

THOMAS MAVROMOUSTAKOS,[1] PETROS CHATZIGEORGIOU,[2] CATHERINE KOUKOULITSA,[1] SERDAR DURDAGI[3]

[1]*Organic Chemistry Laboratory, Chemistry Department, National Kapodistrian University of Athens, Panepistimioupolis-Zographou, Athens 15771, Greece*

[2]*Physical Chemistry Laboratory, Chemistry Department, National Kapodistrian University of Athens, Panepistimioupolis-Zographou, Athens 15771, Greece*

[3]*Institute of Biocomplexity and Informatics, Department of Biological Sciences, University of Calgary, 2500 University Drive, Calgary, AB, Canada T2N 1N4*

Received 20 January 2010; accepted 25 January 2010
Published online 2 June 2010 in Wiley Online Library (wileyonlinelibrary.com).
DOI 10.1002/qua.22610

ABSTRACT: A methodology has been developed to detect partial interdigitation of lipid bilayers when a bioactive molecule is intercalated between the polar, interface, or hydrophobic segments. This methodology uses the easily accessible differential scanning calorimetry (DSC) technique as a screening one and the increase of ΔH due to the incorporated drug in lipid bilayers as a diagnostic thermodynamic parameter. The combined use of X-ray diffraction and Raman spectroscopy complement and confirm the provided by DSC information as it is shown in three classes of molecules, namely AT_1 antagonists, vinca alkaloids, and anesthetic steroids. For the two classes of molecules, AT_1 antagonists and vinca alkaloids, their presence in lipid bilayers results in the increase of ΔH and it is accompanied by the increase of *trans:gauche* ratio and the decrease of *d*-spacing as depicted by Raman spectroscopy and small-angle X-ray diffraction correspondingly, confirming the predictive ability of DSC experiments. When an anesthetic steroid is incorporated in lipid bilayers, neither increase of ΔH nor decrease of *d*-spacing was observed, confirming again the DSC results that show the absence of partial interdigitation of this class of molecules. Molecular dynamics simulations have been carried out for a representative system [(5S)-1-benzylo-5-(1H-benzimidazol-1-ylo-methylo)-2-pyrrolidinone (MMK3) ligands at 1,2-dimyristoyl-sn-glycero-3-phosphocholine (DMPC) lipid bilayer], and the results confirmed the experimental findings. The change of distance at *z*-axis of oxygen atoms at head group of lipid molecule has been measured throughout the simulations. Statistical analysis has shown ~8.8 Å interdigitation. Derived computational results are encouraging and can be performed to another ligand/lipid system. The development of a theoretical methodology will lead to advance the field and save a valuable time and effort. Int J Quantum Chem 111: 1172–1183, 2011

Key words: partial interdigitation; lipid bilayers; DSC; Raman spectroscopy; MD simulation

Correspondence to: T. Mavromoustakos; e-mail: tmavrom@chem.uoa.gr

Introduction

There is a great literature evidence pointing out that interdigitated phase can be induced by bioactive organic molecules when they are incorporated in the lipid bilayers. This interdigitation can be characterized as partial, mixed, or full depending on the extend of the alkyl chain penetration from one alkyl chain to the opposite [1] (Fig. 1). Such molecules include ethanol, benzyl alcohol, vinblastine, vinorelbine, atropine, tetracaine, labdanes, chlorpromazine, MMK3, etc. [2–18] (Fig. 2).

In previous publications, we have pointed out that partial interdigitation can occur in fluid phase and that this interdigitation is caused by molecules characterized as follows: (i) amphiphilic; (ii) preferably bulky; (iii) act on the interface; and (iv) are not very long. Cholesterol is found to break the interdigitation effect as it is very long and it does not allow the alkyl chains of the two layers to interdigitate [6, 8, 9].

To detect the interdigitation in the fluid phase, at least three physical chemical techniques are used in our laboratory: (a) X-ray diffraction experiments using the *d*-spacing (lamellar periodic distance between the bilayers) as a diagnostic factor. However, the decrease of the *d*-spacing in the presence of bioactive material can be attributed to two reasons: (i) due to mesomorphic changes and (ii) interdigitation effect. It is well known that when phospholipids undergo a phase transition from the gel to the liquid crystalline phase, conformational changes occur in the alkyl chain, thus all *trans* conformations are transformed to *gauche* conformations (kinks) that shorten the *d*-spacing. (b) Raman spectroscopy is suitable through measuring the *gauche:trans* ratio and the intermolecular interactions of the opposite acyl chains in the fluid phase to confirm if the decrease of the *d*-spacing is due to mesomorphic changes or interdigitation effects. (c) Differential scanning calorimetry (DSC) is also used as a technique for detecting the interdigitation. The increase of the enthalpy change of the melting curve in the thermal scans due to incorporation of the drug is interpreted as a sign of interdigitation.

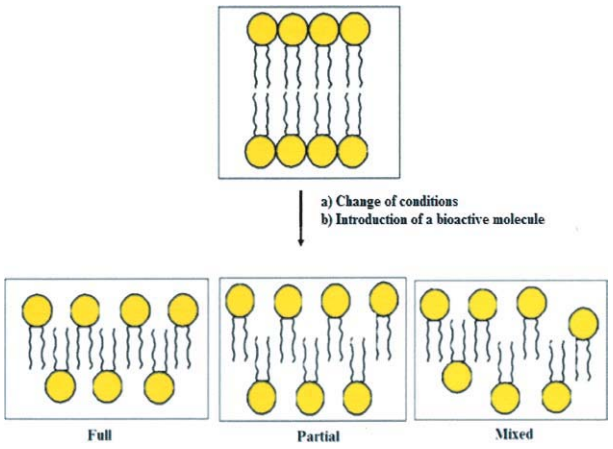

FIGURE 1. Various ways of inducing partial or total interdigitation. [Color figure can be viewed in the online issue, which is available at wileyonlinelibrary.com.]

More specifically, DSC is a suitable, relatively inexpensive technique to study drug to membrane interactions. It has been extensively used to study the thermal properties of phospholipid bilayers [6, 8, 9, and references therein]. For example, the studies of mesomorphic changes of dipalmitoyphosphatidylcholine bilayers have shown that this exists in the gel phase for temperatures lower than 35°C, and in the liquid crystalline phase for temperatures higher than 42°C. The transition is accompanied by several structural changes in the lipid molecules as well as systematic alterations in the bilayer geometry, but the most prominent feature is the *gauche:trans* isomerization taking place in the acyl conformation. The average number of gauche conformers indicates the effective fluidity, which depends on perturbations due to the presence of a drug molecule intercalating between the lipids. Various parameters have been used for interpreting the phase transition, such as the maximum of the phase transition T_m, the onset of the phase transition T_{onset}, and the area of the phase transition ΔH. Among these, ΔH, as it is already mentioned, is the most diagnostic for showing the interdigitation effect. The increase of ΔH is interpreted as a cause of interdigitation effect. Thus, integration of the thermal scans containing phospholipid bilayers alone and drug incorporation will show us the possible interdigitation effect. However, DSC diagnostic parameter ΔH alone cannot show unambiguously the interdigitation effect. Other techniques are used as complementary to confirm this effect.

Raman spectroscopy is one of those techniques that complement DSC data. It is a valuable spectroscopic technique not yet fully explored in the field of drug to membrane interactions. Information concerning the intramolecular interactions in the lipid molecules due to *gauche:trans*

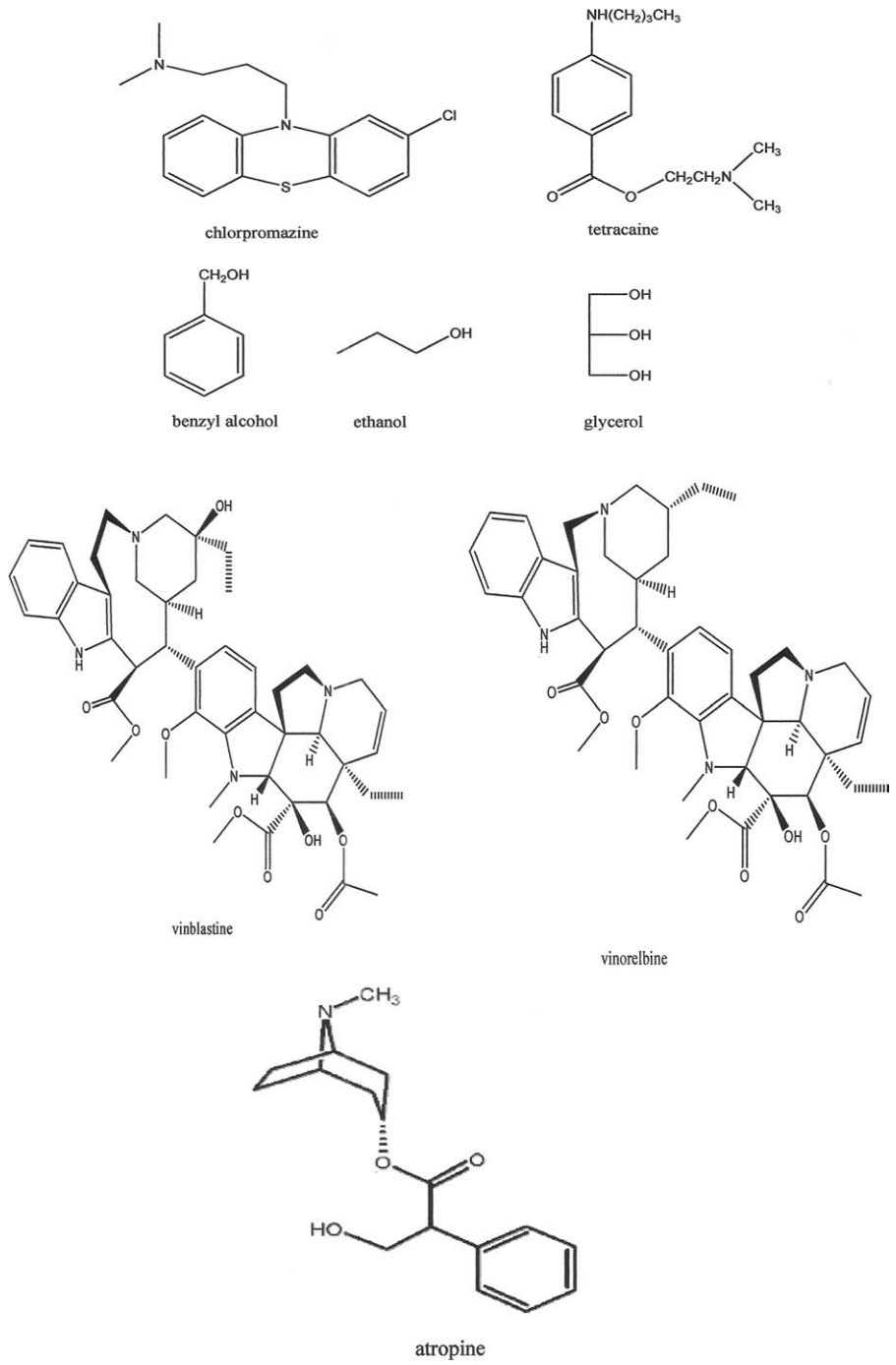

FIGURE 2. Reported molecules that induce interdigitation effects in lipid bilayers.

isomerization as well as the intermolecular acyl-chain interactions of the lipids in the bilayer can be retrieved through Raman spectroscopy. In particular, the intensity of certain bands (2850 cm^{-1}, 2880 cm^{-1}) depicts perturbations of the vibrational modes of the C—H bond evidential to changes in the acyl chain, whereas the intensity of other bands (1090 cm^{-1}, 1130 cm^{-1}) is sensitive to intramolecular changes along the acyl chain, leading to a *gauche:trans* isomerization. In addition, changes on the head group (715 cm^{-1}) in the carbonyl region can also be followed by the Raman

spectroscopy. Raman spectroscopy allows to calculate ΔS and ΔH through Van't Hoff equations. All this valuable information can not only confirm DSC data but also can give a lot of information on the specific interactions of the drug with lipid bilayers. Such detail information is missing from DSC experiments. For example, great difference (7–8 cm^{-1}) of the choline band between the gel to liquid crystalline phase is evident that drug is associated with polar segment and exert electrostatic interactions [2, 19, 20].

A complementary technique and valuable for studying the effect of interdigitation is X-ray diffraction. X-ray diffraction is a very useful and direct method for characterizing materials having periodicity in their structures. Lipid bilayers can be packed into a stack of lamellae which give coherent Bragg-like reflections. Thus, information can be obtained about their structures and about the effects of drugs on the bilayers structure. The periodicity is expressed by the term *d*-spacing. Interdigitation effects cause decrease of *d*-spacing. Therefore, the comparison of *d*-spacing between phospholipid bilayers containing the drug molecule with bilayers absent of drug molecules gives information on the interdigitation effect of drug molecules [21–27].

Materials and Methods

MATERIALS

Phospholipids have been purchased from Avanti Lipids. Anesthetic steroids, alphaxalone (5α-pregnan-16-en-3α-ol-ll,20-dione) and Δ^{16}-alphaxalone (5α-pregn-16-en-3α-ol-ll,20-dione), were kindly donated by Glaxo Research. The rest of the steroids as well as cholesterol were obtained from Sigma, St Louis, MO. Losartan (2-butyl-4-chloro-1-{[2′-(1*H*-tetrazol-5-yl)biphenyl-4-yl]methyl}-(1*H*-imidazol-5-yl)methanol) was kindly donated by Merck. Vinblastine, dimethyl (2*β*,3*β*,4*β*,5α,12*β*,19α)-15-[(5*S*,9*S*)-5-ethyl-5-hydroxy-9-(methoxycarbonyl)-1,4,5,6,7,8,9, 10-octahydro-2*H*-3,7-methanoazacycloundecino [5,4-*b*]indol-9-yl]-3-hydroxy-16-methoxy-1-methyl-6,7-didehydroaspidospermidine-3,4-(dicarboxylate), and vincristine, methyl (1*R*,9*R*,10*S*,11*R*,12*R*,19*R*)-11-(acetyloxy)-12-ethyl-4-[(13*S*,15*S*,17*S*)-17-ethyl-17-hydroxy-13-(methoxycarbonyl)-1,11-diazatetracyclo[13.3.1.$0^{4,12}$.$0^{5,10}$]nonadeca-4(12),5,7,9-tetraen-13-yl]-8-formyl-10-hydroxy-5-methoxy-8,16-diazapentacyclo[10.6.1.$0^{1,9}$.$0^{2,7}$.$0^{16,19}$]nonadeca, were purchased from Sigma Aldrich. All chemicals were used with no further purification.

METHODS

Differential Scanning Calorimetry

Thermal scans were carried out using Perkin-Elmer DSC-7 calorimeter (Norwalk, CT). All samples were scanned from 10 to 60°C until identical thermograms were obtained using a scanning rate of 2.5°C/min. The temperature scale of the calorimeter was calibrated using indium (T_m = 156.6°C) and 1,2-dipalmitoyl-sn-glycero-3-phosphocholine (DPPC) bilayers (T_m = 41.2°C). The following diagnostic parameters were used for the study of drug to membrane interactions: T_m (maximum of the recorded heat capacity), T_{onset} (the starting temperature of the phase transition), and $T_{m1/2}$ (the half-height width of the phase transition). An empty pan for the baseline and a sample containing double-distilled water were run for the temperature range of 10–60°C as a reference for the background. This background was subtracted from each thermal scan of the samples. The area under the observed peak represents the enthalpy change during the transition (ΔH). The mean values of ΔH of three identical scans were tabulated.

Raman Spectroscopy

A portion of the prepared samples (~40 mg) was used for the Raman experiments. The Raman spectra were obtained at 4 cm^{-1} resolution from 100 to 3500 cm^{-1} with an interval of 2 cm^{-1} by using a Perkin-Elmer (Shelton, CT) NIR FT-spectrometer (Spectrum GX II) equipped with a charge-coupled device detector. The measurements were performed at a temperature range of 25–50°C. The temperature was kept constant for 1 h by using a temperature controller from Ventacon (England). The laser power (an Nd:YAG excited at 1064 nm) was kept constant at 400 mW during the measurements. Then, 1500 scans were accumulated, and back-scattering light was collected.

X-ray Diffraction

For the X-ray diffraction experiments, the preparations were deposited on an aluminum foil, dried at 35°C and mounted on a curved glass holder. Small-angle X-ray scattering experiments were performed on an Elliott GX18 generator

TABLE I

The structures of alphaxalone and anesthetic activities of pregane steroids.

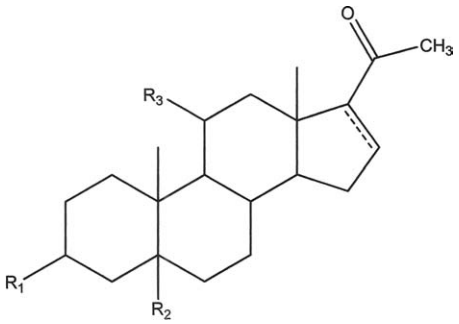

Steroid	R_1	R_2	R_3	16,17 Double bond	Anesthetic activity
1	3βOH	5βH	H_2	No	25
2	3αOH	5βH	H_2	No	3.1
3	3αOH	5αH	H_2	No	3.1
4	3βOH	5αH	H_2	No	100
5	3αOH	5βH	=O	No	6.3
6	3αOH	5αH	=O	No	3.1
7	3βOH	5αH	=O	Yes	Inactive
8	3βOH	5αH	H_2	Yes	Inactive

(Marconi Avionics), equipped with a camera utilizing a single vertical Franks' mirror. Small-angle X-ray diffraction patterns were collected using a Braun position-sensitive proportional counting gas flow detector (Innovative Technology, South Hamilton, MA). During the experiment, we used a helium path for a specimen-to-detector distance of 130 mm and collected the diffraction data with digital accumulations of 1×10^6 to 2×10^6 counts to improve the signal-to-noise ratio. Data were transferred to a VAX computer system, and the intensities were integrated from the computer plots by calculating the area under the diffraction peaks.

Molecular Dynamics Simulations

Molecular dynamics (MD) simulations have been carried out to scan the interdigitation effect at the MMK3/DMPC (1,2-dimyristoyl-sn-glycero-3-phosphocholine/(5*S*)-1-benzylo-5-(1H-benzimidazol-1-ylo-methylo)-2-pyrrolidinone) system. The system includes six MMK3 and 128 DMPC lipids. DMPC lipid bilayer for the MD simulations was obtained from Dr. M. Karttunen's web page [28] (128 DMPC lipids and 3655 water molecules after 20 ns) [29, 30]. The MD simulations were performed with GROMACS 3.3.1 software package [31] using GROMOS96 force field [32]. The simulations were run in the NPT ensemble at 315 K and 1 bar with periodic boundary conditions. During equilibration, the Berendsen barostat and thermostat algorithms were applied [33]. Electrostatic interactions were calculated using the particle mesh Ewald method [34]. Cutoff distances for the calculation of Coulomb and van der Waals interactions were 1.0 and 1.4 nm, respectively. Prior to the dynamics simulation, energy minimization was applied to the full system without constraints using the steepest descent integrator for 2000 steps with the initial step size of 0.01 Å [the minimization tolerance was set to 1,000 kJ/(mol nm)]. The system was then equilibrated via 250 ps simulations with a time step of 2 fs. Finally, a 2.0-ns simulation was performed at 315 K and 1 bar with a time step of 2 fs using Berendsen thermostat and Parrinello-Rahman barostat algorithms [35]. All bonds were constrained using the LINCS algorithm [36]. Visualization of the dynamics trajectories was performed with the Visual Molecular Dynamics software package [37]. Origin 6.0 program [38] was used for the plots.

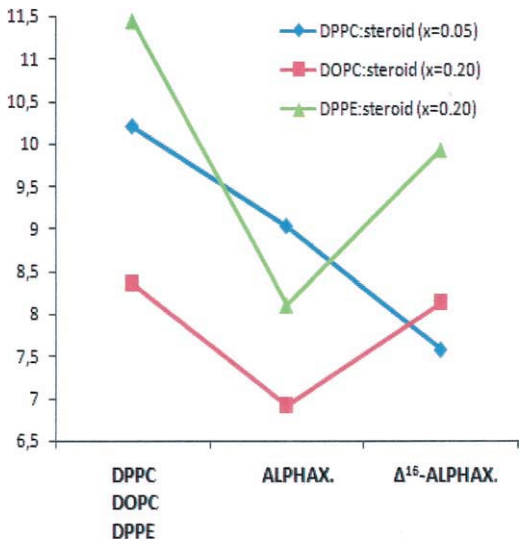

FIGURE 3. ΔH values for the two anesthetic steroids in the three phospholipid bilayer environments. [Color figure can be viewed in the online issue, which is available at wileyonlinelibrary.com.]

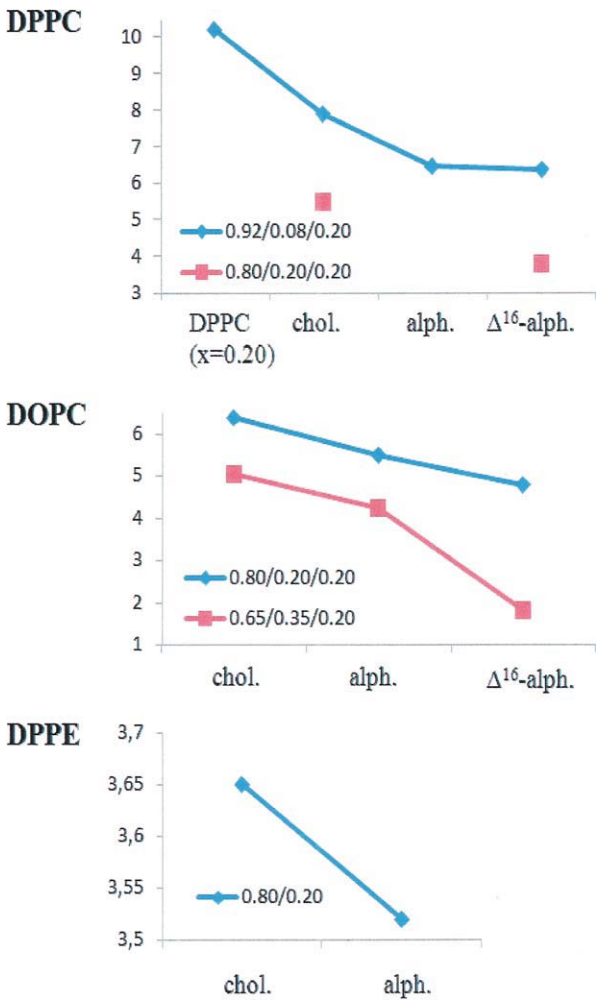

FIGURE 4. ΔH values for the two anesthetic steroids in the three phospholipid bilayer environments containing cholesterol. [Color figure can be viewed in the online issue, which is available at wileyonlinelibrary.com.]

Results and Discussion

We have previously studied AT_1 antagonists, antihypertensive drug molecules that started to be developed two decades ago and known to exert their action in the transmembrane region of lipid bilayers. Because of their amphipathic property, they are expected to act first in the lipid bilayer and then to diffuse to the active site of the receptor. An approach of combining various physical chemical methodologies such as DSC, Raman spectroscopy, and X-ray diffraction is used to investigate their thermal and dynamic properties in lipid bilayers. Our studies depicted that when these molecules are incorporated in the lipid bilayers, they induce partial interdigitation. In particular: (a) they cause increase of ΔH as it is depicted from the integration of the phase transition in calorimetric results; (b) they lower the *gauche:trans* ratio and increase the intermolecular interactions between opposite aliphatic chains as it is shown in Raman spectroscopy; and (c) they are localized at the interface, an ideal topography in the lipid bilayers to form voids in the head-group region and induce partial interdigitation between the lipid layers. This information is derived using a combination of DSC, solid-state NMR, Raman spectroscopy, and X-ray diffraction as well as MD experiments. This effect is related to their drug efficacy as it is reported in our previous study comparing the interdigitation effect in DPPC bilayers using a commercial potent AT_1 antagonist losartan and a synthetic derivative of low-activity MMK3 [(5S)-1-benzylo-5-(1H-benzimidazol-1-ylo-methylo)-2-pyrrolidinone] [19, 22, 39].

In this study, we show additional experimental evidence that confirms our previous approach for detecting the formation of interdigitation. For that reason, we used two classes of molecules, namely anesthetic steroids and vinca alkaloids. Anesthetic steroids are molecules that do not exert interdigitation effect in phospholipid bilayers as they are extensive molecules and are expected to be incorporated in the same way as cholesterol by influencing mainly the alkyl chains of the bilayers [40–43].

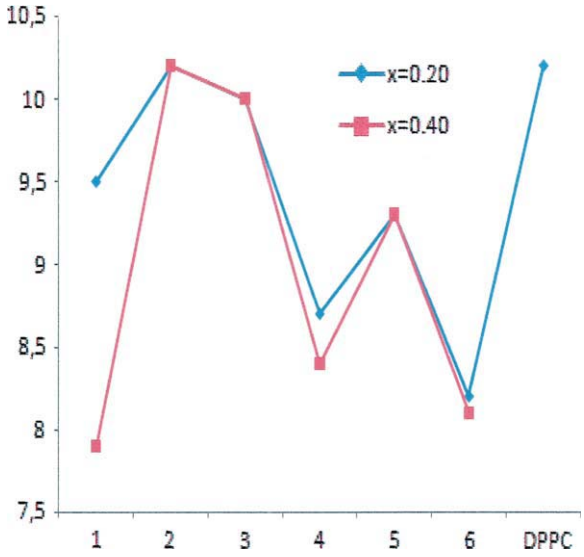

FIGURE 5. ΔH values for a series of anesthetic steroids in the three phospholipid bilayer environments containing cholesterol. [Color figure can be viewed in the online issue, which is available at wileyonlinelibrary.com.]

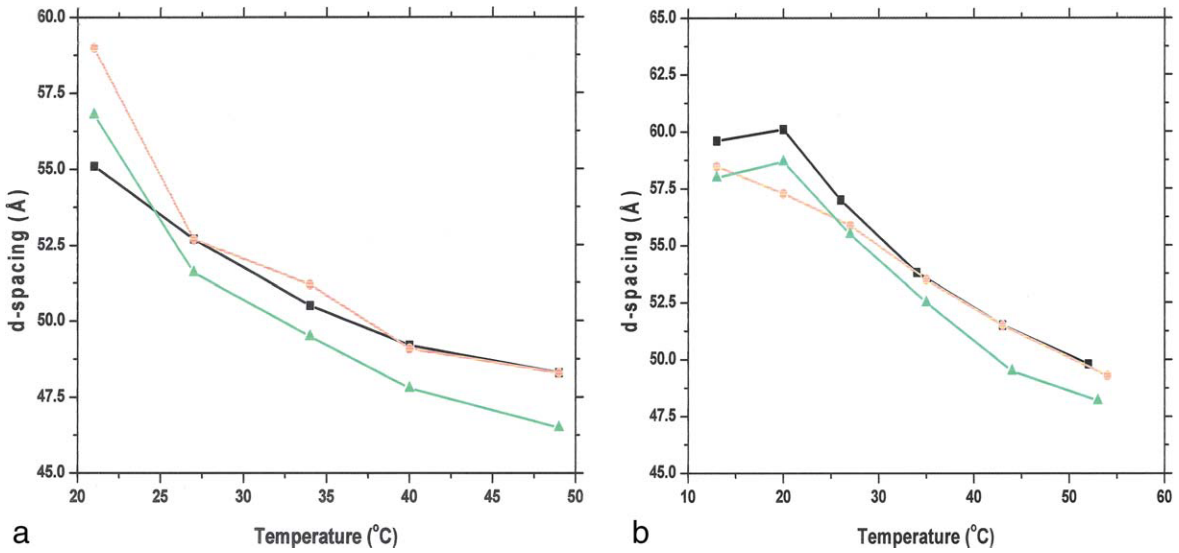

FIGURE 6. (a) *D*-spacing as a function of temperature for DMPC bilayers (squares); DMPC + alphaxalone ($x = 0.15$) (circles) and DMPC + Δ^{16}-alphaxalone ($x = 0.15$) (triangles). (b) *D*-spacing as a function of temperature for DMPC + cholesterol ($x = 0.15$) bilayers (circles); DMPC + cholesterol ($x = 0.15$) + alphaxalone ($x = 0.10$) (squares) and DMPC + cholesterol ($x = 0.15$) + Δ^{16}-alphaxalone ($x = 0.10$) (triangles). [Color figure can be viewed in the online issue, which is available at wileyonlinelibrary.com.]

Contrarily, vinblastine and vincristine, which are vinca alkaloids, are expected to show interdigitation effect in phospholipid bilayers because of their amphiphilic and bulky properties.

We have studied the effect of the anesthetic steroid alphaxalone and its inactive congener Δ^{16}-alphaxalone using DSC as a diagnostic technique (Table I). Thus, ΔH of the main transition was calculated for the two preparations. The value obtained was the mean value for three calculations and did not differ by more than 5%. In our study, the following phospholipids were used: (a) dipalmitoylphosphatidylcholine, a widely used phospholipid that contains symmetric and saturated alkyl chains; (b) dipalmitoylphosphatidylethanolamine that differs from dipalmitoylphosphatidylcholine in the head-group region. It contains ethanolamine instead of choline; (c) dioleoylphosphatidylcholine, a phospholipid that contains a double bond in the alkyl chain between 9 and 10 carbons, characterized by a very low phase transition.

The DSC results on ΔH of the pair of anesthetic steroids at the three different phospholipids are shown in Figure 3. In all cases, the two anesthetic steroids cause the decrease of ΔH, although not very significant at the concentration of $x = 0.20$ molar ratio. Thus, these results do not suggest an interdigitation effect of these steroids on the phospholipid bilayers under study.

The addition of cholesterol in these phospholipids caused a decrease of ΔH in a concentration-dependent condition similar to cholesterol effect. The presence of alphaxalone or Δ^{16}-alphaxalone in phospholipid bilayers containing cholesterol further decreased the enthalpy change (Fig. 4). When the phase transition was significantly

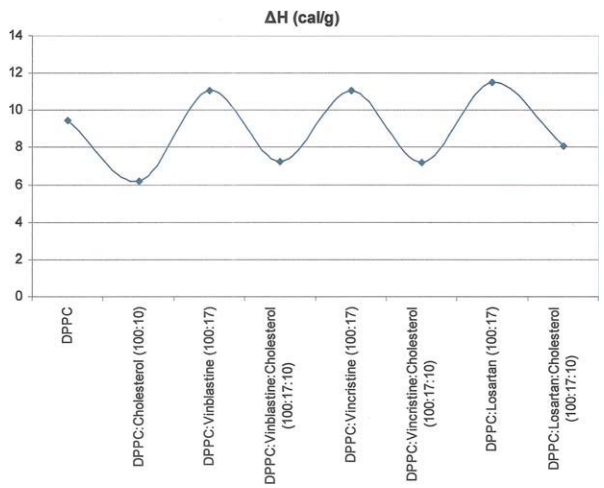

FIGURE 7. ΔH values for the AT_1 antagonist losartan and vinca alkaloids vinblastine and vincristine in the absence and presence of cholesterol. [Color figure can be viewed in the online issue, which is available at wileyonlinelibrary.com.]

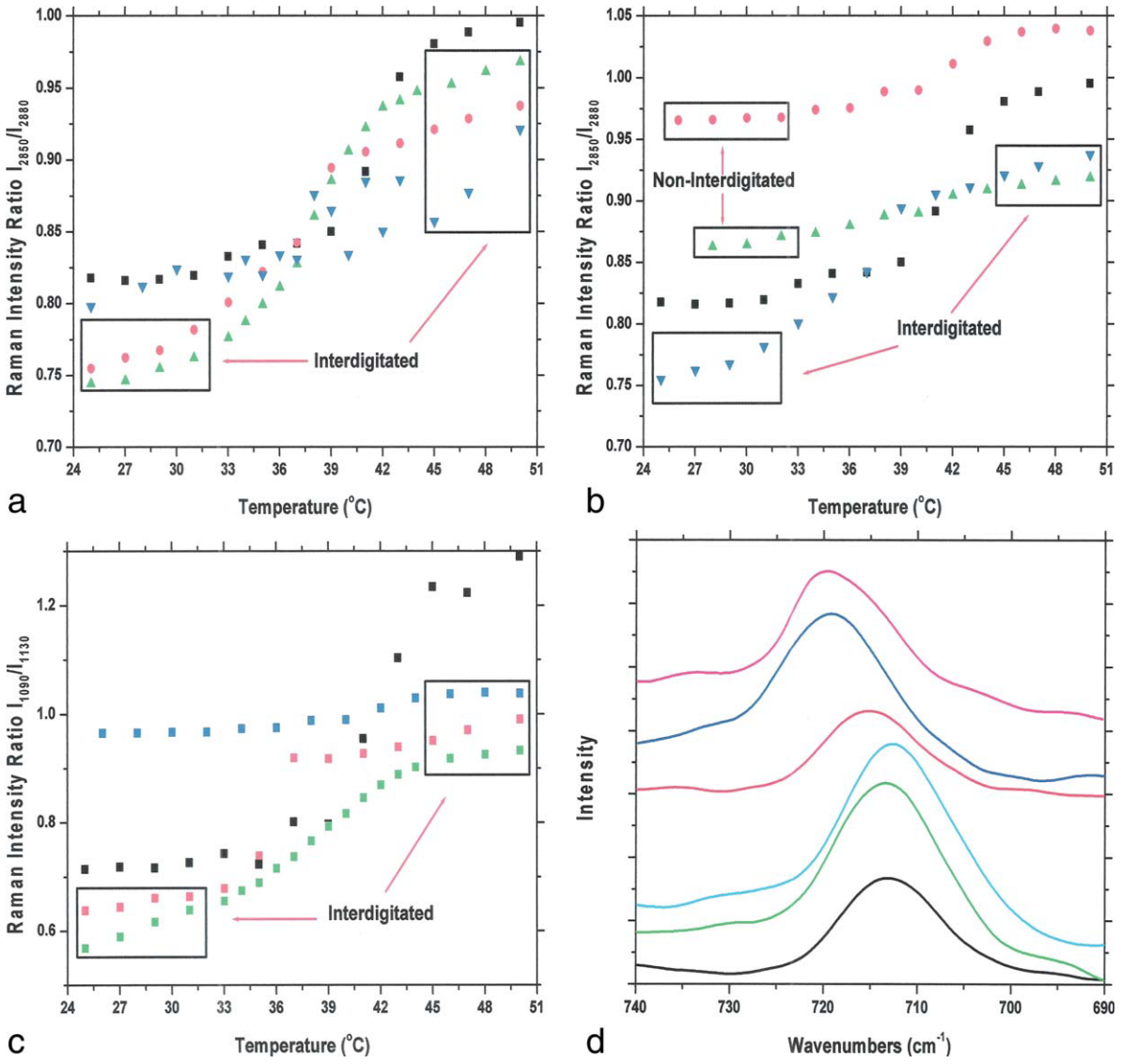

FIGURE 8. (a) Temperature profile of Raman intensity ratio I_{2850}/I_{2880}, which indicates the presence of interdigitated phase in gel and liquid crystalline phase. (Black: DPPC, Red: DPPC/vinblastine 100:17, Green: DPPC/vincristine 100:17, Blue: DPPC/losartan 100:17); (b) Temperature profile of Raman intensity ratio I_{2850}/I_{2880}, which reveals the presence of interdigitated phase (interdigitation) in gel and liquid crystalline phase. (Black: DPPC, Red: DPPC/cholesterol 100:10, Blue: DPPC/vinblastine 100:17, Green: DPPC/vinblastine/cholesterol 100:17:10); (c) Temperature profile of Raman intensity ratio I_{1090}/I_{1130}, which shows the effect of interdigitation in gel and liquid phase. (Black: DPPC, Red: DPPC/vinblastine 100:17, Blue: DPPC/losartan 100:17, Green: DPPC/vincristine 100:17); (d) Raman band at 715 cm^{-1} (C – N stretching of choline) which represents the interactions between vinca alkaloids with the interface. (Black: DPPC at 25 °C, Red: DPPC at 50 °C, Green: DPPC/vinblastine 100:17 at 25 °C, Blue: DPPC/vinblastine 100:17 at 50 °C, Cyan: DPPC/vincristine 100:17 at 25 °C, Magenta: DPPC/vincristine 100:17 at 25 °C). [Color figure can be viewed in the online issue, which is available at wileyonlinelibrary.com.]

broad, no ΔH could be calculated, and therefore some values are missing.

A confirmation of these results was achieved for a series of anesthetic steroids molecules in DPPC bilayers. All the anesthetic steroids run having a wide range of biological activity caused decrease or no change of ΔH (Table I, Fig. 5).

We have run X-ray diffraction experiments in dimyristoylphosphatidylcholine bilayers for alphaxalone and Δ^{16}-alphaxalone in the absence

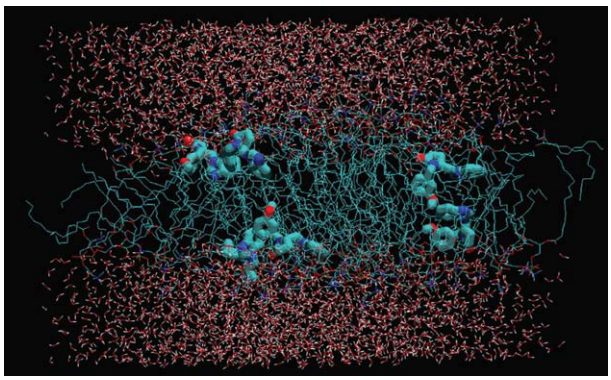

FIGURE 9. The system used for MD simulations included 6 MMK3 and 128 DMPC lipids. DMPC lipid bilayer for the MD simulations was obtained from Dr. M. Karttunen's web page [28] (128 DMPC lipids and 3655 water molecules after 20 ns) [29,30]. [Color figure can be viewed in the online issue, which is available at wileyonlinelibrary.com.]

[Fig. 6(a)] and presence of cholesterol [Fig. 6(b)]. We observed that for the DMPC preparations containing Δ^{16}-alphaxalone, the *d*-spacing in the liquid crystalline phase was identical to that of the control DMPC preparation, whereas the *d*-spacing of DMPC containing the anesthetic steroid alphaxalone was always smaller by 1.5 Å because of its more liquid state at the corresponding temperatures. The addition of Δ^{16}-alphaxalone in DPPC preparation containing cholesterol ($x = 0.15$) again did not change the *d*-spacing. The addition of the active analog as it is expected reduced it insignificantly.

Also, the interactions between vinca alkaloids, vinblastine and vincristine, with DPPC bilayers were examined at $x = 0.17$ molar ratio of the drugs. The influence of these molecules on ΔH values are shown in Figure 7 and are compared with those of AT_1 antagonist, losartan. The presence of vinca alkaloid incorporated in DPPC bilayers shows about 17% increase in ΔH values, like that caused by losartan which is 21%. This increase is an evidence of the formation of the partial interdigitated phase in the gel phase $P_{\beta I}$. The addition of $x = 0.10$ molar ratio of cholesterol decreases the value of ΔH to about 35% as it is expected in all cases, because cholesterol is a known molecule that disturbs the creation of interdigitation effect (Fig. 7).

For a more detailed analysis of the formation of the interdigitation, Raman spectroscopy was used on these samples for monitoring the *gauche:trans* isomerization and the intermolecular interactions between opposite acyl chains. We have calculated the Raman intensity ratio I_{1090}/I_{1130}, which constitutes a direct measurement of *gauche* and *trans* population, and Raman intensity ratio I_{2850}/I_{2880}, which reflects the intermolecular interactions. In addition, changes in the head group region were obtained by analysis of the C—N band. The obtained results are shown in Figure 8(a–d).

Figure 8(a) represents the peak height intensity ratio I_{2850}/I_{2880} for DPPC bilayers containing either vinblastine or vincristine or losartan at $x = 0.17$ molar ratio. The lower the ratio is, the greater are the interactions between the opposite alkyl chains. In general terms, the value of the ratio I_{2850}/I_{2880} in all temperatures of loaded DPPC samples is lower than the correlated value of unloaded DPPC sample, an observation that reveals the formation of interdigitation in both gel and liquid phase. The addition of $x = 0.10$ molar ratio cholesterol in the previous samples increases the value of this ratio in gel phase, indicating that cholesterol prevents the formation of interdigitation at temperatures below melting points. However, at temperatures above melting points, there is no effect on these values, demonstrating that the presence of an interdigitated liquid phase is not affected by cholesterol [Fig. 8(b)].

Concerning the intramolecular interactions, the high peak intensity ratio I_{1090}/I_{1130} was studied, which reflects the *gauche:trans* isomerization. Figure 8(c) shows that the presence of vinblastine or vincristine at $x = 0.17$ in DPPC bilayers decreases the value of this ratio in liquid phase in the same pattern as losartan when compared with unloaded DPPC's values, reflecting the presence of interdigitation phenomenon in liquid phase. These results again show the similar behavior of these drugs in inducing interdigitation at the liquid phase.

Figure 8(d) presents the shift of the band C—N, which reveals the electrostatic interactions between the examined molecules with the interface of the bilayers. In unloaded DPPC, this band shifts at about 2 cm^{-1}, whereas in the cases of vinblastine and vincristine, this band shifts at about 6 cm^{-1}, and in losartan at about 8 cm^{-1}. These results show that these molecules affect in a similar way as the head-group region of the DPPC bilayers. It appears that DSC can be a predictive methodology for the partial interdigitation effect. DSC results for the molecules losartan, vinblastine, and vincristine published to exert interdigitation effect in DPPC bilayers are shown to increase ΔH in the absence of

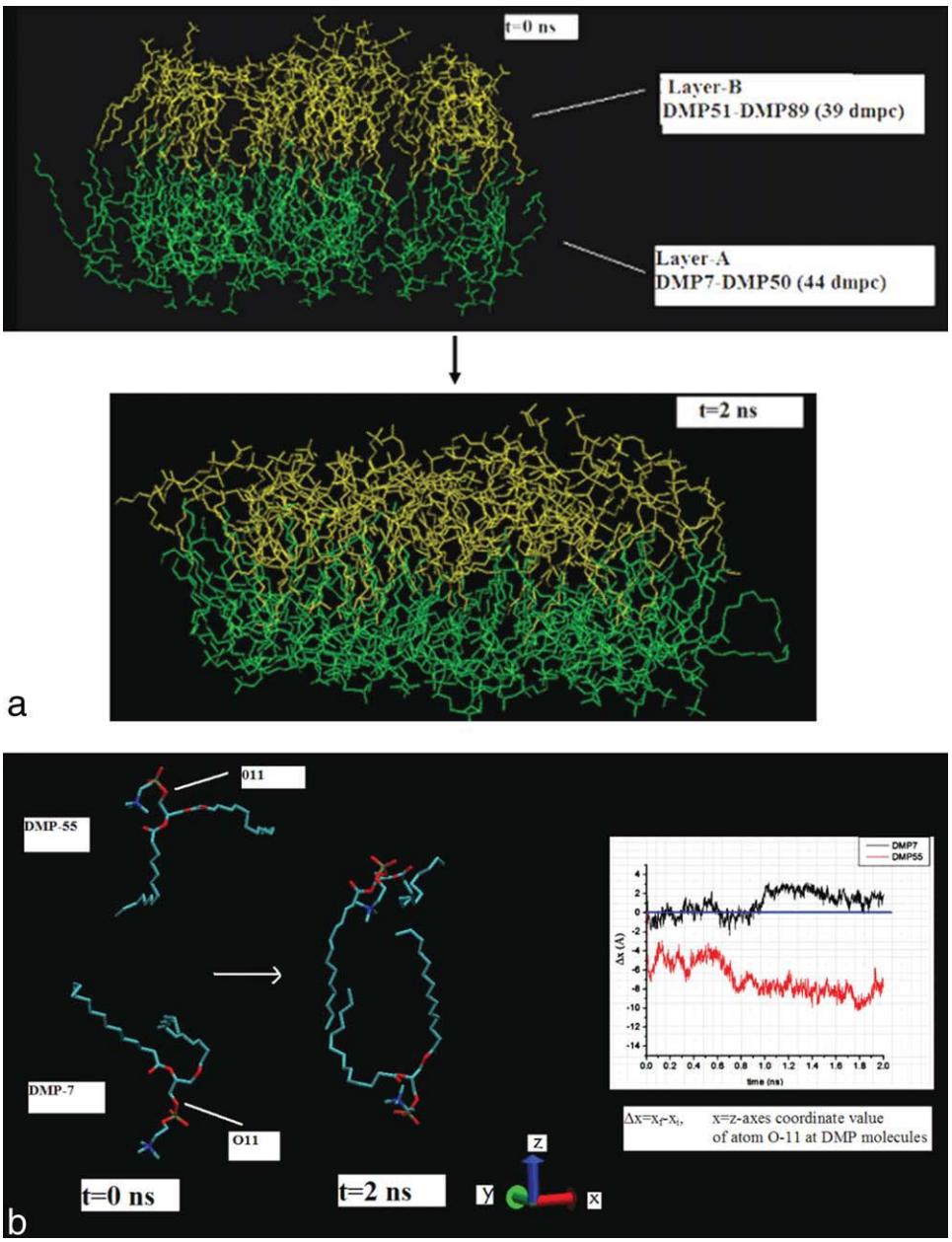

FIGURE 10. (Top) Poses at $t = 0$ ns and $t = 2$ ns of MD simulations for DMPC bilayers containing 6 MMK3 molecules (3 for layer A and 3 for layer B). DMP7-DMPC50 presents the 44 DMPC lipids of layer A and DMP51-DMPC89 presents the 39 DMPC lipids of layer B. (Bottom) Change of distance at *z*-axis of oxygen atom at head group (labeled as O11) has been measured throughout the simulations. Representative figure for DMP-7 at layer A and DMP-55 at layer B shows clearly that oxygen atom position at DMP-7 was increased (+*z*-axis about 2 Å) whereas corresponding oxygen atom position at DMP-55 was decreased (−*z* axis about 6 Å). Thus an interdigitation has been occurred with around 8 Å. [Color figure can be viewed in the online issue, which is available at wileyonlinelibrary.com.]

cholesterol. When cholesterol is present, they oppose the effect of the decrease of ΔH observed by cholesterol (Fig. 7). More detail experiments are under progress for providing more evidence to the above obtained results.

MD simulations have been applied at DMPC bilayers including MMK3. To clearly see the effects of molecules to interdigitation, the six MMK3 molecules (instead of one) are inserted in DMPC bilayers, as shown in Figure 9. Interdigitation has

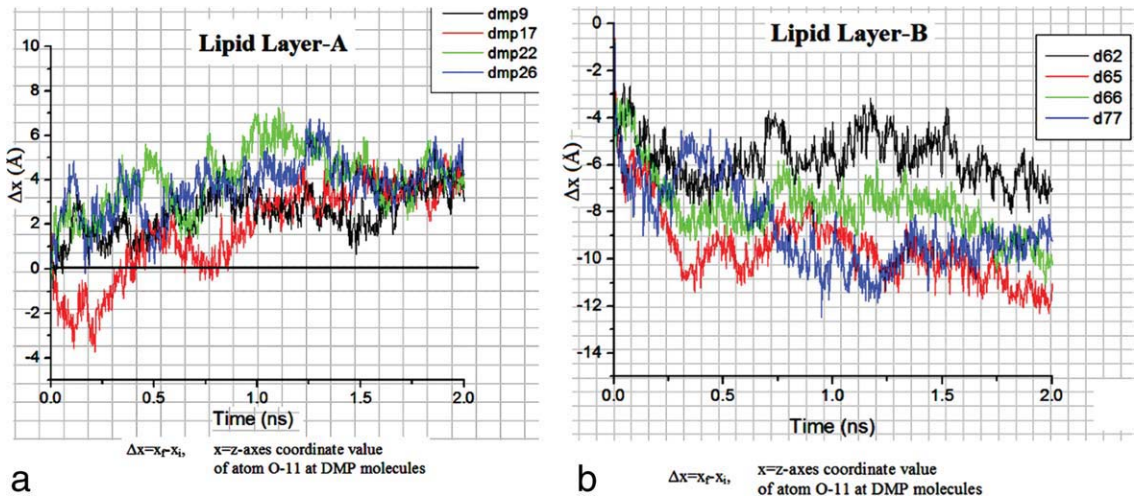

FIGURE 11. Statistical analysis for 83 DMPC lipids showed that oxygen atom (O11) has been shifted 1.96 Å (in $+z$ axis) at layer A and 6.86 Å (in $-z$ axis) at layer B. Thus, 8–9 Å interdigitation has been occurred (for clarity, only a few lipids from layers A and B were presented). [Color figure can be viewed in the online issue, which is available at wileyonlinelibrary.com.]

been scanned with the change of coordinates at head group oxygens. Specifically, the change of distance at z-axis of oxygen atom at head group (labeled as O11) has been measured throughout the simulations (Fig. 10). Representative figure for DMP-7 at layer A and DMP-55 at layer B clearly shows that oxygen atom position at DMP-7 was increased ($+z$ axis about 2 Å), whereas corresponding oxygen atom position at DMP-55 was decreased ($-z$ axis about 6 Å). This analysis has been repeated for all other lipids used in the simulations. These results showed that the observation for DMP-7 and DMP-55 is similar for other DMPC lipids at layers A and B (Fig. 11).

A statistical analysis for all DMPC lipids at layers A and B used in MD simulations was performed. The results showed that oxygen atom (O11) has been shifted 1.96 Å in $+z$-axis (average value out of 44 DMPC) at layer A and 6.86 Å in $-z$ axis (average value out of 39 DMPC) at layer B. Thus, ~8.8 Å interdigitation has been occurred.

Although experiments can provide a fairly complete description of an interdigitation, such experiments usually require a great deal of effort and it is difficult to be performed routinely. Similar information on interdigitation may be obtained more easily using molecular modeling techniques such as MD simulations, which have become feasible during the last decade attributed to the rapid growth in computational power. To our knowledge, this is the first attempt using in silico techniques on examination of partial interdigitation of lipid bilayers. The obtained computational results are very encouraging and they may open a new avenue for entire investigation of interdigitation. Thus, questions such as which kind of molecules enhance the interdigitation and which ones do not, and how cholesterol molecules at lipid bilayers affect the interdigitation can be successfully addressed.

Conclusions

We have shown that DSC, a simple thermodynamic technique, can be predictive for showing partial interdigitation. The thermodynamic parameter used for the prediction of partial interdigitation is the increase of enthalpy change when the additive drug is incorporated in lipid bilayers. Confirmation of the predictive power of DSC can be realized using a combination of X-ray diffraction experiments along with Raman spectroscopy.

We have shown that for AT_1 antagonists, the increase of ΔH is accompanied by the decrease of d-spacing and the increase of *trans:gauche* isomerization. Anesthetic steroids do not show increase of ΔH and they have been shown to not decrease d-spacing by small X-ray diffraction. Thus, in this case, X-ray results are in agreement with DSC data. Vinca alkaloids, vinblastine and vincristine, have shown to increase ΔH in DSC experiments.

Indeed, Raman spectra show increase of *trans:-gauche* ratio, and preliminary small-angle X-ray results show that these vinca alkaloids decrease the *d*-spacing values. In conclusion, all three experimental methodologies can be used as complementary to reveal partial interdigitation.

MD simulations can be applied for observing the partial interdigitation eminent in the experimental results used in the above mentioned methodologies. Thus, a direct measurement of the displacement of the terminal alkyl segment due to the presence of drug molecule can be used. These theoretical calculations will make faster the understanding of the stereoelectronic requirements for partial interdigitation.

References

1. Slater, J. L.; Huang, C. H. Prog Lipid Res 1988, 27, 325.
2. O'Leary, T. J.; Levin, I. W. Biochim Biophys Acta 1984, 776, 185.
3. O'Leary, T. J.; Ross, P. D.; Levin, I. W. Biophys J 1986, 50, 1053.
4. Auger, M.; Smith, I. C. P.; Jarrell, H. C. Biochim Biophys Acta 1989, 981, 351.
5. Löbbecke, L.; Cevc, G. Biochim Biophys Acta 1995, 1237, 59.
6. Koukoulitsa, C.; Kyrikou, I.; Demetzos, C.; Mavromoustakos, T. Chem Phys Lipids 2006, 144, 85.
7. Cunningham, B. A.; Lis, L. J. Biochim Biophys Acta 1986, 861, 237.
8. Maswadeh, H.; Demetzos, C.; Daliani, I.; Kyrikou, I.; Mavromoustakos, T.; Tsortos, A.; Nounesis, G. Biochim Biophys Acta 2002, 1567, 49.
9. Kyrikou, I.; Daliani, I.; Mavromoustakos, T.; Maswadeh, H.; Demetzos, C.; Xatziantoniou, S.; Giatrellis, S.; Nounesis, G. Biochim Biophys Acta 2004, 1661, 1.
10. McIntosh, T. J.; McDaniel, R. V.; Simon, S. A. Biochim Biophys Acta 1983, 731, 109.
11. Demetzos, C.; Matsingou, C. Chem Phys Lipids 2007, 145, 45.
12. Nerdal, W.; Gundersen, S. A.; Thorsen, V.; Heiland, H.; Holmen, H. Biochim Biophys Acta 2000, 1464, 165.
13. Hao, Y.; Xu, Y.; Chen, J.; Huang, F. Biochim Biochem Biophys Res Commun 1998, 245, 439.
14. Gjerde, A. U.; Holmsen, H.; Nerdal, W. Biochim Biophys Acta 2004, 1683, 28.
15. Cao, A.; Brachet, E. H.; Azize, B.; Taillanlier, E.; Perret, G. Chem Phys Lipids 1991, 58, 225.
16. Banuelos, S.; Arrono, J. L.; Cavaves, R. J. M.; Ferragut, J. A.; Muga, A. Eur J Biochem 1993, 213, 1269.
17. Attal, Y.; Co, X. A.; Perret, G.; Tailandier, E. Chem Pharm Bull 1997, 45, 1317.
18. Nguyen, T. S.; Weers, P. M. M.; Raussens, V.; Whang, Z.; Ren, G.; Sulehek, T.; Hoeprich, P. D.; Ryan, R. O. Biophys Biochim Acta 2008, 1778, 303.
19. Fotakis, C.; Christodouleas, D.; Chatzigeorgiou, P.; Zervou, M.; Benetis, N. P.; Viras, K.; Mavromoustakos, T. Biophys J 2009, 96, 2227.
20. Kyrikou, I.; Xadjikakou, S.; Kovala-Demertzi, D.; Viras, K.; Mavromoustakos, T. Chem Phys Lipids 2004, 132, 157.
21. Mavromoustakos, T.; Papahatjis, D.; Laggner, P. Biochim Biophys Acta 2001, 1512, 183.
22. Mavromoustakos, T.; Yang, D. P.; Broderick, W.; Fournier, D.; Herbette, L. G.; Makriyannis, A. Pharmacol Biochem Behav 1991, 40, 547.
23. Yang, D. P.; Mavromoustakos, T.; Beshah, K.; Makriyannis, A. Biochim Biophys Acta 1992, 1103, 25.
24. Yang, D. P.; Mavromoustakos, T.; Makriyannis, A. Life Sci 1993, 53, 117.
25. Mavromoustakos, T.; Yang, D. P.; Charalambous, A.; Herbette, L. G.; Makriyannis, A. Biochim Biophys Acta 1990, 1024, 336.
26. Mavromoustakos, T.; Yang, D. P.; Makriyannis, A. Biochim Biophys Acta 1995, 1237, 183.
27. Rappolt, M.; Laggner, P.; Pabst, G. In Recent Research Developments in Biophysics Part II; Pandalai, S. D., Ed.; Transworld Research Network: Trivandrum, 2004; Vol. 3, 363.
28. Karttunen, M. SoftSimu. Available at: http://www.apmaths.uwo.ca/~mkarttu/downloads.shtml. Accessed on January 8, 2009.
29. Patra, M.; Karttunen, M.; Hyvonen, M.; Falck, E.; Lindqvist, P.; Vattulainen, I. Biophys J 2003, 84, 3636.
30. Patra, M.; Karttunen, M.; Hyvonen, M.; Falck, E.; Lindqvist, P. J Am Chem Soc 2004, 108, 4485.
31. van Der Spoel, D.; Lindahl, E.; Hess, B.; Groenhof, G.; Mark, A. E.; Berendsen. H. J. J Comput Chem 2005, 26, 1701.
32. Van Gunsteren, W. F.; Billeter, S. R.; Eising, A. A.; Hunenberger, P. H.; Kruger, P.; Mark, A. E.; Scott, W. R. P.; Tironi, I. G. Biomolecular Simulation: The GROMOS96 Manual and User Guide; Vdf Hochschulverlag AG an der ETH Zurich: Zurich, 1996.
33. Berendsen, H. J. C.; Postma, J. P. M.; van Gunsteren, W. F.; DiNola, A.; Haak, J. R. J Chem Phys 1984, 81, 3684.
34. Essmann, U.; Perera, L.; Berkowitz, M. L.; Darden, T.; Lee, H.; Pedersen, L. G. J Chem Phys 1995, 103, 8577.
35. Parrinello, M.; Rahman, A. J Appl Phys 1981, 52, 7182.
36. Hess, B.; Bekker, H.; Berendsen, H. J. C.; Fraaije, J. G. E. M. J Comput Chem 1997, 18, 1463.
37. Humphrey, W.; Dalke, A.; Schulten, K. J Mol Graphics 1996, 14, 33.
38. Microcal Products. Available at: http://www.microcal.com. Accessed on January 8, 2009.
39. Zoumpoulakis, P.; Daliani, I.; Zervou, M.; Kyrikou, I.; Siapi, E.; Lamprinidis, G.; Mikros, E.; Mavromoustakos, T. Chem Phys Lipids 2003, 125, 13.
40. Mavromoustakos, T.; Yang, D. P.; Makriyannis, A. Biochim Biophys Acta 1994, 1194, 69.
41. Mavromoustakos, T.; Yang, D. P.; Makriyannis, A. Biochim Biophys Acta 1995, 1239, 257.
42. Mavromoustakos, T.; Theodoropoulou, E.; Yang, D. P. Biochim Biophys Acta 1997, 1328, 65.
43. Makriyannis, A.; Yang, D. P.; Mavromoustakos, T. In Steroids and Neuronal Activity—Ciba Foundation Symposium No. 153; Wiley: London, 1990; p 172.